DENTAL MATERIALS XXX (2016) XXX–XXX

Available online at www.sciencedirect.com

ScienceDirect

journal homepage: www.intl.elsevierhealth.com/journals/dema

Analysis of titanium and other metals in human jawbones with dental implants – A case series study

Xiuli He[a,b], Franz-Xaver Reichl[a,b], Yan Wang[a,b], Bernhard Michalke[c], Stefan Milz[d], Yang Yang[a,b], Philipp Stolper[e], Gabriele Lindemaier[f], Matthias Graw[f], Reinhard Hickel[b], Christof Högg[a,b,*]

[a] Department of Operative/Restorative Dentistry, Periodontology and Pedodontics, Ludwig-Maximilians-University of Munich, Goethestr. 70, 80336 Munich, Germany
[b] Walther-Straub-Institute of Pharmacology and Toxicology, Ludwig-Maximilians-University of Munich, Nussbaumstr. 26, 80336 Munich, Germany
[c] Research Unit Analytical Biogeochemistry, Helmholtz Zentrum Munich – German Research Center for Environmental Health (GmbH), Ingolstaedter Landstraße 1, 85764 Neuherberg, Germany
[d] Department of Anatomy II – Neuroanatomy, Ludwig-Maximilians-University of Munich, Pettenkoferstr. 11, 80336 Munich, Germany
[e] Fogra Forschungsgesellschaft Druck e.V., Streitfeldstr 1, 81673 Munich, Germany
[f] Institute of Forensic Medicine, Ludwig-Maximilian-University of Munich, Nussbaumstr. 26, 80336 Munich, Germany

ARTICLE INFO

Article history:
Received 27 October 2015
Received in revised form
23 December 2015
Accepted 31 May 2016
Available online xxx

Keywords:
Titanium content
Human jawbones
Dental implants
Ti particles

ABSTRACT

Objective. The aim of this study was to measure titanium (Ti) content in human jawbones and to show that Ti was released from dental implants inserted into these jawbones.
Methods. Seven samples from four human subjects with dental implants were analysed as test group and six bone samples of similar topographical regions from six human subjects without implants served as control. The contents of various elements in human jawbones were detected by inductively coupled plasma optical emission spectrometry. The distributions of various isotopes in human mandibular bone were measured with laser ablation-inductively coupled plasma-mass spectrometry (LA-ICP-MS). Histological analyses of undecalcified, Giemsa-Eosin stained mandible sections were performed by light microscopy and particles were identified in human bone marrow by scanning electron microscope-energy dispersive X-ray analysis.
Results. In test group only Ti content was significantly higher compared to control group. The mean contents of Ti were 1940 μg/kg in test group and 634 μg/kg in control group. The highest Ti content detected in human mandibular bone was 37,700 μg/kg-bone weight. In samples 4–7 (human subjects II–IV), increased Ti intensity was also detected by LA-ICP-MS in human mandibular tissues at a distance of 556–1587 μm from implants, and the intensity increased with decreasing distance from implants. Particles with sizes of 0.5–40 μm were found in human jawbone marrow tissues at distances of 60–700 μm from implants in samples 4–7.

* *Corresponding author at*: Department of Operative/Restorative Dentistry, Periodontology and Pedodontics, LMU Munich, Goethestr. 70, 80336 Munich, Germany. Tel.: +49 89 2180 73842; fax: +49 89 2180 73841.
E-mail address: christof.hoegg@lrz.uni-muenchen.de (C. Högg).
http://dx.doi.org/10.1016/j.dental.2016.05.012

Please cite this article in press as: He X, et al. Analysis of titanium and other metals in human jawbones with dental implants – A case series study. Dent Mater (2016), http://dx.doi.org/10.1016/j.dental.2016.05.012

Significance. Ti released from dental implants can be detected in human mandibular bone and bone marrow tissues, and the distribution of Ti in human bone was related to the distance to the implant.

1. Introduction

In the last 50 years titanium (Ti) and its alloys have been widely used for dental and medical applications [1,2]. Clinically, pure Ti (Ti >99%) and the alloy Ti-6Al-4V are mainly used for endosseous implants [2]. Ti alloys with other metals (e.g. nickel (Ni), chromium (Cr), iron (Fe), and molybdenum (Mo)) are applied for implant devices such as bone plates or screws [2,3]. Ti is the main component in those implants/implant devices so that a stable TiO_2 layer [4,5] on the surface can provide Ti based implants/implant devices with a high biocompatibility and resistance to corrosion [6–9].

Although Ti based implants have been considered to be biological inert, it has been found that implants in the body can undergo corrosion and release particulate debris over time [10,11]. It has been reported that the metallic debris from Ti based implants might exist in several forms including particles (micrometer to nanometre size), colloidal and ionic forms (e.g. specific/unspecific protein binding) [12,13], organic storage forms (e.g. hemosiderin, as an iron-storage complex), inorganic metal oxides and salts [12]. According to a previous study [14], the degradation of implants in the human body is primarily induced by wear and corrosion: wear is the mechanical/physical form of implant degradation which produces particles; while corrosion refers to the chemical/electrochemical form of degradation that mainly produces soluble metal ions [14]. Ti particles released from implants have been found in the regenerated bone and peri-implant tissues in animals [7,15]. It has been shown that also Ti ions can be released from embedded implants in animals [16,17]. Ti particles/ions are able to enter the circulation of blood and lymph [12,18,19]. Ti particles detached from hip, knee and mandible implants have been detected in organs such as liver, spleen, lung and lymph nodes [5,19]. Increased levels of elementary Ti have also been detected in the blood of patients with poorly functioning implants [12].

Increased concentrations of metals (e.g. Ti, Cr, Co and Al) derived from implants in body fluids might induce acute or chronic toxicological effects [12]. The long-term effects of Ti derived from implants are still not fully understood, but associated hypersensitivity and allergic reactions in patients have been reported [20,21]. In a clinical study, 0.6% of 1500 patients were found to exhibit Ti allergic reactions [20]. Additionally, it has been found that detached metal debris from implants might cause marrow fibrosis, necrosis and granulomatosis [22–24].

The aim of our study was to measure the release of Ti and other metallic elements from dental implants through detailed post-mortem studies of human subjects with dental implants. In the present study, Ti released from implants inserted into human jawbones was identified and quantified, and the spatial distribution of Ti in human jawbones near implants was also investigated.

2. Materials and methods

2.1. Materials

The test group contained 7 samples from four human subjects with dental implants (Table 1). The control group contained 6 bone samples from similar topographical regions from six human subjects without dental implants.

The bodies were individually donated for medical research. Subjects I–III in the test group and all six of the subjects from the control group were obtained during the dissection course of the anatomical institute of the Ludwig-Maximilian-University Munich. Bone implant sample from subject IV was supplied by the institute of forensic medicine of the Ludwig-Maximilian-University Munich. Subjects I–III carried two implants (one on each side of the mandible) replacing the mandibular canine teeth (FDI System: 33, 43). Subject IV carried two implants that replaced the left first and second molars in the mandible (FDI System: 36 and 37). All the lower jawbones in the test group contained no additional natural teeth. Four out of the six control subjects were toothless as well. The other two control subjects were partially edentulous. The average age of the subjects in the test group (excluding subject IV) and control group were 88 and 85 years, respectively.

For subjects I–III, each of the two implants with the adjacent jawbone was taken as a single sample; for subjects IV, two implants with adjacent jawbone on each side were taken as a single sample. Therefore, there were seven implant samples in our experiment (Table 1). Implants used in samples 5–6 were produced by Astra Tech implant system (Mannheim, Germany), and the implants used for sample 4 and sample 7 were produced by Straumann AG (Basel, Switzerland). The manufacturers of the implants of samples 1–3 were unknown. Due to ethical consideration, it is not possible to get more information about the implants, such as the "age" of the implants (for how many years it has been loaded), the type of the implants and the surface treatment on the implants. Ti dental implants have no identification number to provide detail information (e.g. for age determination).

2.2. Sample analysis by inductively coupled plasma optical emission spectrometry (ICP-OES)

2.2.1. Sample preparation

All 7 samples of test group and all 6 samples of control group had been fixed in 4% buffered formalin (Merck, Darmstadt, Germany). The soft tissue was cautiously removed

Please cite this article in press as: He X, et al. Analysis of titanium and other metals in human jawbones with dental implants – A case series study. Dent Mater (2016), http://dx.doi.org/10.1016/j.dental.2016.05.012

Table 1 – Summary information for the test group.

Subject number	Age	Gender	Implants	Sample number	
No. I	98	Female	2 pieces, on the positions of both of the both mandibular canine teeth (FDI System: 33, 43)	No. 1: right mandible segment	No. 2: left mandible segment
No. II	83	Female	2 pieces, on the positions of both of the mandibular canine teeth (FDI System: 33, 43)	No. 3: left mandible segment	No. 4: right mandible segment
No. III	84	Male	2 pieces, on the positions of both of the mandibular canine teeth (FDI System: 33, 43)	No. 5: right mandible segment	No. 6: left mandible segment
No. IV	Unknown	Female	2 pieces, on the positions of the left first and second molars in the lower jaw (FDI System: 36 and 37)	No. 7: left Mandible segment	

with Feather® disposable stainless steel scalpels and then immersed in 100% methanol (Carl Roth, Karlsruhe, Germany).

2.2.1.1. *Test group*. Jawbone slices in the sagittal plane were prepared from samples 1–7 by cutting with a diamond band saw (cut-grinder macro, patho-service GmbH, Oststeinbek, Germany). The samples were cut at intervals of 1 mm in a direction moving toward the implants, and cutting was stopped immediately adjacent to the implant (Fig. 1). From each sample, at least 5 jawbone slices with an approximate thickness of 500 μm were obtained. For analysis the 5 jawbone slices closest to the implant were used.

Each jawbone slice was further divided into 4 quadrants (A–D) (Fig. 1). Each quadrant was weighed and dissolved in 1 ml sub-boiled distilled nitric acid at 170 °C for 12 h. The solution was subsequently diluted (1:5) in Milli-Q Water. The contents of the elements Ti, Al, Cd, Cr, Co, Cu, Fe, Mn, Mo, Ni and V in each quadrant were analysed by ICP-OES (Optima 7300 DV, Perkin Elmer, Rodgau-Jügesheim, Germany). The remaining specimens containing the implant and adjacent bone were reserved for further analysis (Sections 2.3 and 2.4).

2.2.1.2. *Control group*. Control samples were taken from mandibular regions topographically comparable to those bearing the implants. Again 5 adjacent jawbone slices were cut and each of the slices was divided into 4 quadrants. For analysis by ICP-OES, same procedure as samples 1–7 was performed.

2.2.2. *Analytical procedure*

An ICP-OES, Optima 7300 DV system (Perkin Elmer, Rodgau-Jügesheim,Germany) was used for element determination. Sample introduction was carried out using a peristaltic pump connected to a Seaspray nebulizer with a cyclon spray chamber. The measured spectral element lines were (in nm): Al: 167.078, Cd: 214.438, Cr: 267.716, Co: 228.616, Cu: 324.754, Fe: 259.941, Mn: 257.611, Mo: 202.030, Ni: 231.604, V: 292.464, Ti: 334.941.

The RF power was set to 1400 W; the plasma gas was 13 L Ar/min, whereas the nebulizer gas was approximately 0.6 L Ar/min after daily optimization.

Routinely each ten measurements, three blank determinations and a control determination of a certified standard for all mentioned elements were performed. Calculation of results was carried out on a computerized lab-data management system, relating the sample measurements to calibration curves, blank determinations, control standards and the weight of the digested sample.

The volumes of sample digests were sufficient for duplicate measurements ($n = 2$).

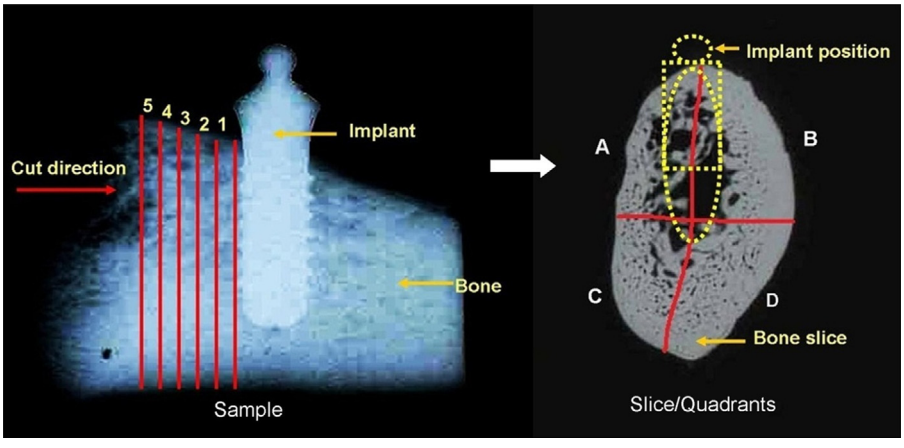

Fig. 1 – Scheme (X-ray image) of the cutting procedure for samples 1–7: at least five bone slices were obtained from each sample; each slice was divided into 4 quadrants (A, B, C and D). The red lines represent the cuts, and the distance between two cuts is 1 mm, the numbers represent slice numbers, number 1 represents the slice closest to implant. (For interpretation of the references to colour in this figure legend, the reader is referred to the web version of this article.)

Please cite this article in press as: He X, et al. Analysis of titanium and other metals in human jawbones with dental implants – A case series study. Dent Mater (2016), http://dx.doi.org/10.1016/j.dental.2016.05.012

2.2.3. Calculations and statistics

For a total jaw bone slice the content (μg/kg) of each investigated element was calculated by dividing the summed concentrations of the 4 quadrants with their summed masses.

The results are presented as mean ± standard error of the mean (SEM). Independent two-sample *t*-test and a one-way ANOVA analysis followed by post hoc Bonferroni adjustment were performed for statistical analysis. Differences were considered statistically significant only when the *p*-value was less than 0.05 ($p < 0.05$) [25].

2.3. Content distribution measured by Laser Ablation-Inductively Coupled Plasma-Mass Spectrometry (LA-ICP-MS)

2.3.1. Sample preparation

The remaining parts of samples 4–7 (the bone surrounding the implants) and bone samples from the control group were dehydrated in ascending ethanol fractions (70%, 80%, 90% and 100%), defatted in xylene (Merck, Darmstadt, Germany), and embedded in methylmethacrylate (Fluka, Switzerland). Samples 4–7 were analysed because in these samples significantly higher Ti contents (compared to controls) were detected with ICP-OES measurement in Section 2.2.

Details of the embedding and cutting process can be found in a previous study [26]. The polymerized methacrylate blocks were cut at a thickness of approximately 300 μm parallel to the long axis of the implants in the mesio-distal plane using a Leica SP 1600 saw-microtome (Leica, Wetzlar, Germany). The sections were used for spectroscopy and for histological analysis.

The distribution of the isotopes ^{47}Ti, ^{27}Al, ^{43}Ca, ^{52}Cr, ^{59}Co, ^{63}Cu, ^{57}Fe, ^{39}K, ^{55}Mn, ^{60}Ni, ^{51}V, ^{64}Zn and ^{66}Zn in each section were analysed by Laser Ablation-Inductively Coupled Plasma-Mass Spectrometry (LA-ICP-MS) – NWR-213® (New Wave Research Co. Ltd.) coupled to a NexION® 300 ICP-MS (PerkinElmer).

2.3.2. Analytical procedure

The laser ablations started from the bone region at a distance of 5 mm from the implant and ended in the implant region. In this manner, sample-specific backgrounds could be measured by moving from low to high contents [27], and memory effects were avoided. Two to three parallel ablation lines with each time 6 measurements into the deep (10 μm depth ablation per measurement) were performed for each jawbone slice. The average value of 2–6 measurements was calculated for each line (the first measurement was discarded in order to eliminate possible contamination on the surface of the bone sections which could have occurred during the cutting process). Instrument settings and parameters are shown in Table 2.

After the laser ablations, contact radiographs (Faxitron X-ray Corporation, Lincolnshire, IL, USA) for each section were taken on Agfa Strukturix X-ray sensitive film (Agfa-Gevaert, Mortsel, Belgium). The laser lines were clearly visible on the X-ray film and were photographed with an Axiophot microscope (Zeiss, Goettingen, Germany), equipped with Zeiss Plan-Neofluar objectives (5× and 10×) in transmitted light mode.

Table 2 – Instrument settings for LA-ICP-MS.

Laser	Energy: 0.930 mJ Power: 100% Pulse repetition rate: 10 Hz Scan speed: 35 μm/s Spot size: 50 μm Ablation pattern: line Depth: approx. 10 μm
ICP	Plasma power: 1200 W Transport gas: 1.2 L/min Ar Auxiliary gas: 0.8 L/min Ar Cool gas: 17 L/min Ar
MS	Registered isotopes: ^{47}Ti, ^{27}Al, ^{43}Ca, ^{52}Cr, ^{59}Co, ^{63}Cu, ^{57}Fe, ^{39}K, ^{55}Mn, ^{60}Ni, ^{51}V, ^{64}Zn and ^{66}Zn Dwell time/isotope: 25 ms

2.4. Histological analysis

2.4.1. Sample preparation

From each of the samples 4–7, one of the sections (cutting procedure described in Section 2.3.1) was glued (Cyanolit 201, Panacol LTD., Zürich, Switzerland) on opaque plastic slides, ground thinner, polished (EXAKT® 400CS grinding system, EXAKT Vertriebs GmbH, Norderstedt, Germany) and stained with Giemsa-Eosin stain (Sigma Aldrich, Steinheim, Germany).

The same procedure was applied for the control samples.

2.4.2. Light microscopy observation and scanning electron microscope-energy dispersive X-ray (SEM-EDX) measurements

The stained sections were examined with an Axiophot microscope (Zeiss, Goettingen, Germany) that was equipped with Zeiss Plan-Neofluar objectives (5× and 10×) in transmitted light mode. Images were recorded with an Axciocam HRc digital camera (Zeiss, Goettingen, Germany).

The sections that contained visible dark particles were coated with gold and investigated with a SEM (EVD MA 15) equipped with secondary electron (SE) and back-scattered electron (BSE) detectors. The energy dispersive X-ray (EDX) analyses were performed using an Oxford INCA Penta Fetx 3.

The samples of the control group were also histologically investigated, coated with gold and analysed by SEM-EDX.

3. Results

3.1. Sample analysis by ICP-OES

Among all the investigated elements (Ti, Al, Cd, Cr, Co, Cu, Fe, Mn, Mo, Ni and V), only the element Ti in the test group (samples 1–7) showed significantly higher content compared to the control group ($p < 0.05$).

Ti contents of each total jawbone slice from samples 1–7 and control group are shown in Fig. 2. The highest Ti content (13,205 μg/kg-bone weight) of all slices was detected in sample 6. The average Ti content across all 35 bone slices ($n = 35$) of samples 1–7 (1940 ± 469 μg/kg-bone weight) was significantly higher compared to the average content across the 30 bone slices ($n = 30$) from the control group (634 ± 58 μg/kg-bone weight).

Please cite this article in press as: He X, et al. Analysis of titanium and other metals in human jawbones with dental implants – A case series study. Dent Mater (2016), http://dx.doi.org/10.1016/j.dental.2016.05.012

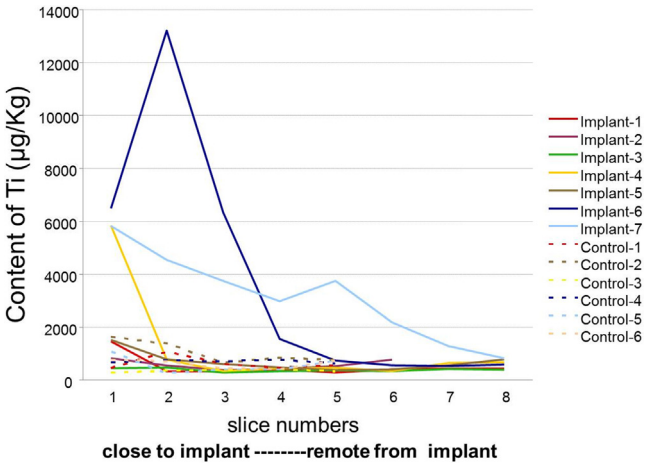

Fig. 2 – Ti contents in the total bone slices from implant samples 1–7 and all control samples. The X-axis represents the number of bone slices; the interval between each two numbers is 1 mm. The Y-axis represents the contents of Ti measured in each total bone slice.

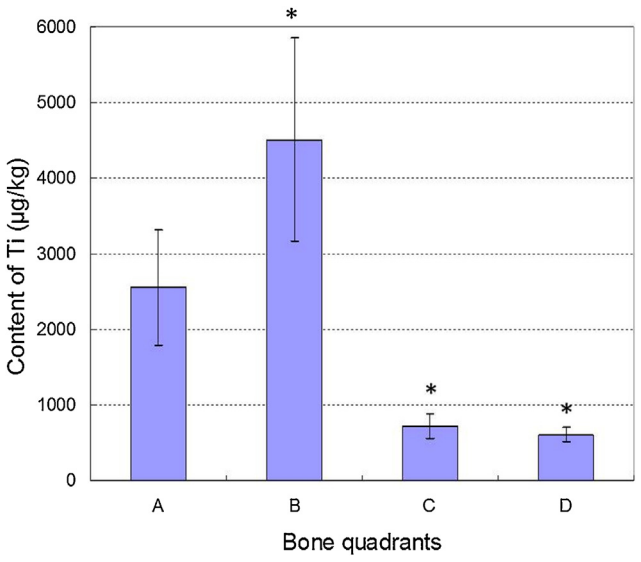

Fig. 4 – The average Ti contents of 4 quadrants of all bone slices from 7 samples in test group (mean ± SEM), $^{*}p < 0.05$.

Ti contents of the total jawbone slices with approximately the same distance from the implant (distance identified by same slice numbers) of all 7 samples are shown in Fig. 3 (mean ± SEM). There were no significant differences in Ti content averages between slices obtained at different distances from the implants ($p > 0.05$).

The average Ti contents for each of the four quadrants (samples 1–7) are shown in Fig. 4. Quadrant B in slice 2 of sample 6 showed the highest Ti content (37,700 µg/kg-bone weight) compared to all the other single quadrants (Fig. 5). The sum of the average Ti contents in the upper half of the bone slice – quadrants A + B (7064 ± 1932 µg/kg-bone weight) – is significantly higher compared to the sum of the average Ti contents in the lower half of bone slice – quadrants C + D (1327 ± 256 µg/kg-bone weight) (Fig. 6). Within the control group there were no significant differences of the Ti contents calculated for all combinations of quadrants or slices.

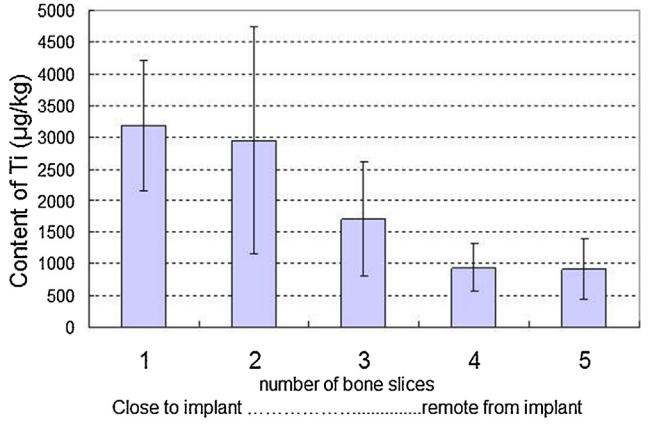

Fig. 3 – Ti contents in each total bone slice in various distances to implants, the x-axis represents the number of bone slices, the interval between each two numbers is 1 mm, and error bars represent the SEMs.

3.2. *Distribution of isotopes measured by LA-ICP-MS*

The isotopes ^{47}Ti, ^{27}Al, ^{43}Ca, ^{52}Cr, ^{59}Co, ^{63}Cu, ^{57}Fe, ^{39}K, ^{55}Mn, ^{60}Ni, ^{51}V, ^{64}Zn and ^{66}Zn in the bone slices with longitudinal cuts through the implants of samples 4–7 (which showed higher Ti content compared to control group measured by ICP-OES) were detected by LA-ICP-MS. Qualitative results are shown in Table 3. ^{47}Ti was the only isotope of all investigated isotopes that could be detected in implant and human jawbone/jawbone marrow tissue of samples 4–7 (with implant) but not in the control samples without implants.

For samples 4–7 along the ablation lines different intensities of ^{47}Ti were detected. In sample 4 the distribution of ^{47}Ti along one ablation line showed that the average ^{47}Ti intensity in a bone region within about 966 µm from the implant is 14 times higher compared to average value of bone at a distance >966 µm from the implant. Samples 5–7 showed comparable

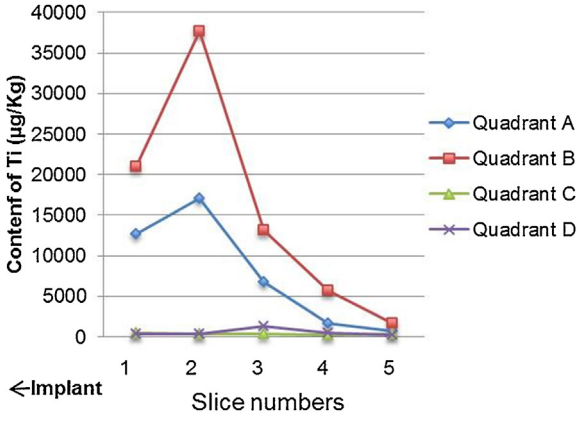

Fig. 5 – Ti contents in 4 quadrants of all slices in sample 6, slice numbers 1–5 represent all slices analyzed in sample 6, number 1 represents the slice closest to implant.

Please cite this article in press as: He X, et al. Analysis of titanium and other metals in human jawbones with dental implants – A case series study. Dent Mater (2016), http://dx.doi.org/10.1016/j.dental.2016.05.012

Table 3 – The distribution of the isotopes measured by LA-ICP-MS in the detected bone slices.

Sample numbers	Isotopes in implants (>99%)	Isotopes in bone/bone marrow tissues
4	^{47}Ti (94%), ^{52}Cr (4%), ^{55}Mn (0.55%), ^{56}Fe (0.52%), ^{60}Ni (0.42%)	^{27}Al, ^{39}K, ^{43}Ca, ^{47}Ti, ^{53}Cr, ^{64}Zn, ^{66}Zn
5	^{47}Ti (94.8%), ^{27}Al (4.5%), ^{51}V (0.23%), ^{52}Cr (0.14%)	^{27}Al, ^{39}K, ^{43}Ca, ^{47}Ti, ^{53}Cr, ^{64}Zn, ^{66}Zn
6	^{47}Ti (98.2%), ^{27}Al (0.68%), ^{52}Cr (0.16%)	^{27}Al, ^{39}K, ^{43}Ca, ^{47}Ti, ^{53}Cr, ^{64}Zn, ^{66}Zn
7	^{47}Ti (93.7%), ^{27}Al (5.3%), ^{52}Cr (0.25%), ^{60}Ni (0.21%)	^{27}Al, ^{39}K, ^{43}Ca, ^{47}Ti, ^{64}Zn, ^{66}Zn
Control	–	^{27}Al, ^{39}K, ^{43}Ca, ^{53}Cr, ^{64}Zn, ^{66}Zn

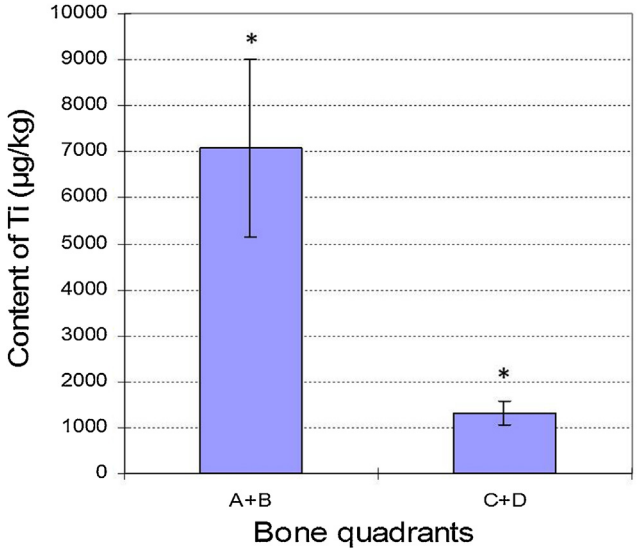

Fig. 6 – The average Ti contents in the upper part (A + B) and lower part (C + D) of each slice in the test group. The error bar represents the SEM, $^{*}p < 0.05$.

results for ^{47}Ti: increased intensities of ^{47}Ti were also detected at distances nearer than 556–1587 μm to the implant surfaces.

Fig. 7 shows the X-ray image of the ablation line in the bone slice of sample 4 combined with LA-ICP-MS results (distributions of ^{43}Ca and ^{47}Ti).

3.3. *Histological analyses*

The histological analysis was performed for samples 4–7 and the control group. Continuous bone contact with the implant surface was observed for sample 4 and sample 5 by light microscopy, while observation of samples 6 and 7 showed only bone implant contact at isolated spots. Observation of samples 4–7 by light microscopy revealed black dots between the cells of the bone marrow tissue, which were identified as Ti particles by SEM-EDX analysis. Primary location of Ti particles was in the bone marrow tissue at a distance of 60–700 μm from the implant, with particle sizes <40 μm (Fig. 8a and b). Fig. 8c shows multinucleated cells in the bone marrow tissues near implant. Local avital bone regions were identified in Fig. 8d by the absence of cell nuclei throughout the lacunae of the mineralized tissue. Fig. 8e reveals traces of marrow fibrosis, an indication of previous inflammatory reactions. No Ti particles, no signs of fibrosis, no avital bone tissue and no multinucleated cells were found in the control group (Fig. 8f).

Results of Ti particle identification by SEM-EDX are shown in Fig. 9a–c. Ti particle size measurement revealed sizes from 0.5 to 5 μm (detection limitation of SEM for magnification factor used in present method is 0.5 μm).

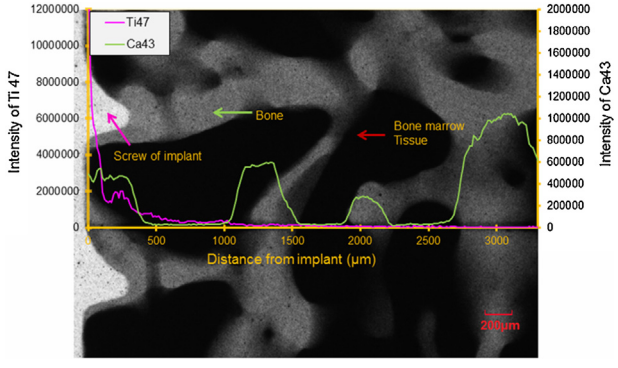

Fig. 7 – X-ray image of one laser ablation line (the part near implant) in sample 4 combined with LA-ICP-MS result (implant screw = white, bone = gray, bone marrow tissues = black).

4. Discussion

In this study, Ti released from dental Ti implants in human jawbones was measured and identified with ICP-OES, SEM-EDX and LA-ICP-MS. It is very rare to get human jawbones with dental implants. Within 4 years only 7 samples with jaw Ti-implants have been obtained from four human individuals from the anatomical institute and forensic medicine institute of the Ludwig-Maximilians-University Munich. This is the first study investigating Ti release from dental implants in human jawbone.

Due to ethical considerations and privacy protection it is not possible to get more information about the implants, such as the "age" of the implants (for how many years it has been loaded), the type of the implants, the method of surgeon and surface treatment of the implants and impurities present in the implant before insertion. Furthermore, the research in this study is focused on the Ti release from Ti implants in human jawbones compared to controls without Ti implants. Therefore, influences of factors like "age" or "type of implants", etc. play no role for this research. The individuals in the test and the control groups examined in the present study were highly comparable with respect to age and gender distribution.

4.1. *ICP-OES*

Among the analysed elements Ti, Al, Cd, Cr, Co, Cu, Fe, Mn, Mo, Ni and V, only Ti showed significantly higher contents in the test group compared to the control group.

Ti is commonly used for dental implants [6], and it has already been found that Ti particles can be released into the

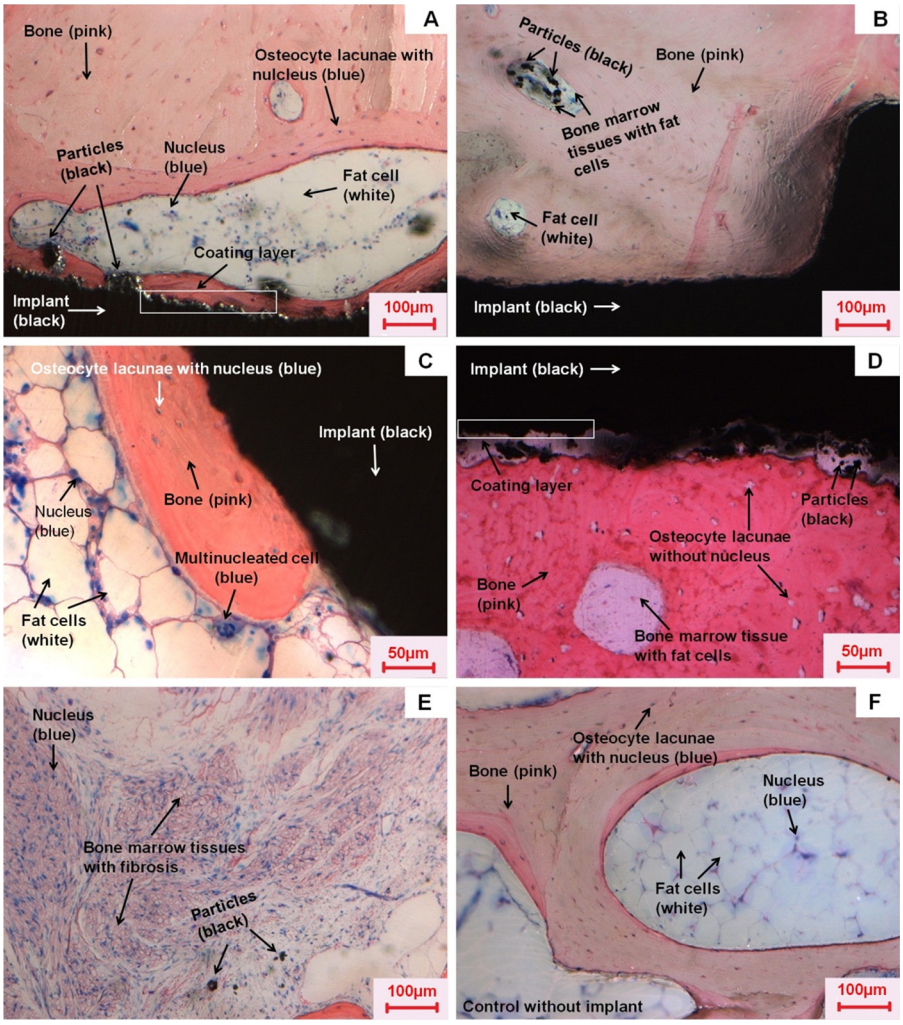

Fig. 8 – The histological images of bone slices with/without implants. Slices (300 μm thick) were glued on opaque plastic slides, ground thinner, polished and stained with Giemsa-Eosin. (a) Bone slice image taken in the combination of transmitted light mode and reflected light mode, a coating layer (marked in rectangle) at the implant surface could be observed with oblique reflected light, particles are visible in bone marrow tissues. The coated implant has a good contact with bone. (b) Particles could be found in bone marrow tissues containing fat cells, and are further identified by SEM-EDX (shown in Fig. 9). The implant has a good contact with bone. (c) Bone slice with multinucleated cell (cell with more than one nucleus) in the bone marrow tissues near the implant. (d) Bone slice with avital bone marrow tissues (identified by the absence of nuclei in the osteocyte lacunae) near the implant. A coating layer (marked with a rectangle) could also be observed. (e) Bone slice with fibrosis in the bone marrow tissues near the implant. (f) Bone slice without implant (control). Fat cell = white, nucleus = blue, particle = black, bone marrow tissues (consist of cells) = white, bone = pink. (For interpretation of the references to colour in this figure legend, the reader is referred to the web version of this article.)

bone tissues from implants [2,14,15]. However, there are less data about the absolute and relative Ti content in human bone surrounding dental implants.

A previous study showed that maximal 4000 μg/kg-bone weight of Ti in rat tibia bone tissues with Ti implant could be detected by ICP-MS after 10 weeks implantation [28]. In the present study, the average content of Ti in the test group measured by ICP-OES (1940 μg/kg-bone weight) was 3 times higher compared to the control group. The highest Ti content of all bone quadrants was 37,700 μg/kg-bone weight. According to previous studies [29,30], Ti particles (<150 μm) exhibited no cytotoxicity in human fibroblasts [29,30], but 10 μg/ml of TiO_2 Nanoparticles (NPs) with a size of 30 nm induced 40% reductions in the cell viabilities of human amnion epithelial cells [30]. Additionally, previous study of our group showed that the EC_{50} of Ti microparticles (<44 μm) in PDL-hTERT cells was above 999 mg/ml, while the EC_{50} of Ti nanoparticles (NPs) (20–250 nm) was 2.84 mg/ml [31]. Regarding the highest Ti content (37,700 μg/kg), the following calculation for rough risk assessment can be given: assuming that Ti in 1 kg bone corresponds to Ti in 1 L fluid, a maximal Ti concentration of 38 μg/ml can be calculated. This value is 3.8 times higher compared to

Please cite this article in press as: He X, et al. Analysis of titanium and other metals in human jawbones with dental implants – A case series study. Dent Mater (2016), http://dx.doi.org/10.1016/j.dental.2016.05.012

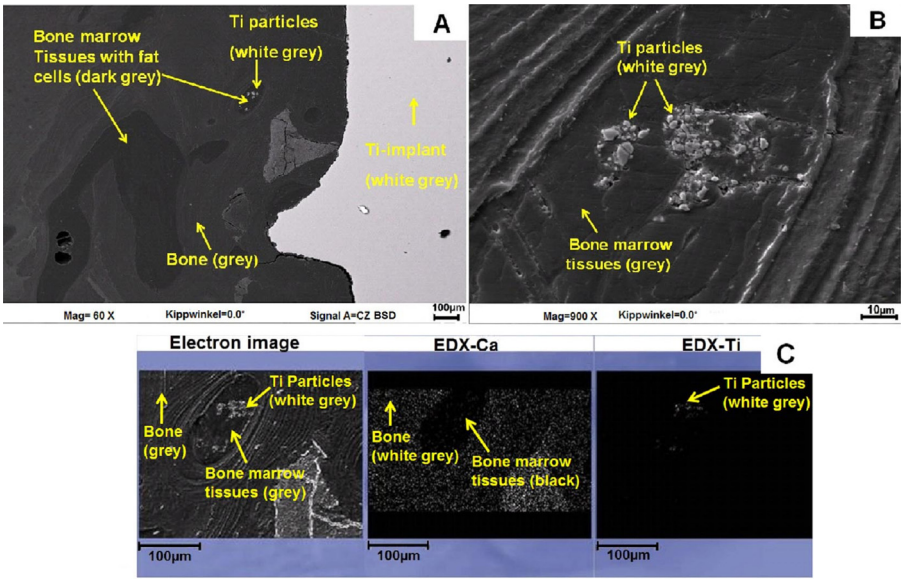

Fig. 9 – SEM image and EDX analysis of the section with particles in Fig. 8(b). (a) Backscattered (BSD) SEM image: Ti implant = white gray, particles = white gray, bone marrow tissues = dark gray, bone = gray. (b) Magnification of the region with particles shown in (a) by SEM. Particles (white gray) could be visualized inside the bone marrow tissues (gray). (c) EDX analysis of the region with particles in (a). On the left is the SEM image of the detected region, in the middle is the intensity of Ca in detected region (bone = gray, bone marrow tissue = black), and on the right is the intensity of Ti in detected region (Ti particles = white gray). The particles in the bone marrow tissues in Fig. 8(b) are identified as Ti particles.

reported cytotoxic concentration (10 μg/ml) of TiO_2 NPs [30] and 74 times lower compared to the EC_{50} (2.84 mg/ml) of Ti NPs [31].

ICP-OES results revealed no distance-dependence of the ^{47}Ti distributions in the total jawbone slices (slice 1–5) of each sample, but the ^{47}Ti contents in the upper quadrants A + B of the bone slices in test group were 5-time higher compared to the lower quadrants C + D. The bone quadrants A + B are anatomically regarded as the alveolar bone, which is known to have a remodeling behavior reacting very sensitive to the transmitted load. Previous studies also reported that the maximum stress (e.g. masticatory forces) is distributed around the implant neck which is surrounded by alveolar bone [32,33]. Obviously, this might explain the higher ^{47}Ti content in the upper quadrants in the current study. Moreover, the main part of the implant is anchored in the upper part of the jawbone, so the upper quadrants A + B of the bone slices are closer to the implant compared to the lower quadrants C + D, and this shorter distance to implant may result in the higher ^{47}Ti content as well. Additionally, the upper quadrants might receive a considerable particle load during the insertion of the implant, which could also lead to higher ^{47}Ti content in the upper quadrants.

4.2. LA-ICP-MS

Due to its flexible spatial analysis capability and high sensitivity, LA-ICP-MS is applied to measure elements, such as Ca, Mg and Sr in bones [27,34]. Moreover, this technique is able to detect unique elemental distributions in micro-spatial areas of dental tissues [35]. In the present study, LA-ICP-MS was used to analyse the region immediately adjacent to the implant because bone slice samples in this region cannot be obtained by the cutting method used for ICP-OES.

The distributions of 13 isotopes ^{47}Ti, ^{27}Al, ^{43}Ca, ^{52}Cr, ^{59}Co, ^{63}Cu, ^{57}Fe, ^{39}K, ^{55}Mn, ^{60}Ni, ^{51}V, ^{64}Zn and ^{66}Zn in bone samples 4–7 with implants were measured by LA-ICP-MS. In bone samples without implant no increased ^{47}Ti was detected. Increased intensity of ^{47}Ti for samples 4–7 was detected in the bone region adjacent to the implant (about 556–1587 μm away from the implant surface). In a previous study, Ti particles from the implant were found in the peri-implant sheep tissue at a distance >200 μm from the implant [15]. Obviously, Ti can migrate from the implant into the surrounding human jawbone or jawbone marrow tissues. In addition, the intensity of ^{47}Ti increased with decreasing distance from the implants, which suggests that the distribution of ^{47}Ti in the jawbone depends on the distance from the implant. This finding is consistent with the ICP-OES results showing that Ti content in upper quadrants A + B (closer to the implant) is significantly higher compared to the lower quadrants C + D. The lack of observations of distance-dependence across the total bone slices by ICP-OES might be attributable to the cutting method not being able to obtain jawbone slices that were sufficiently close to the implant.

^{43}Ca can be taken as an indicator of bone [27]. In this study, ^{43}Ca distribution along the ablation line in the bone slices is shown. Interestingly, ^{47}Ti is present not only in the peri-implant human jawbone marrow tissues but also in the cortical or trabecular bone matrix adjacent to the implant. This is in agreement with previously reported results showing

that Ti particles are found not only in peri-implant animal tissues but also in the bone close to the implants [7,15].

4.3. *Histological analyses*

In the present study, the light microscopy and SEM-EDX results show that Ti particles (0.5–40 μm) are present in human jawbone marrow tissues at a distance of 60–700 μm from the implant. Nearly identical results have been shown by the following studies: Ti particles (from the implant surface) were able to be found in the peri-implant sheep tissue at a distance >200 μm from the implant [15]; Ti particles could not only be observed in peri-implant tissues but also in newly formed bone [7,15]. It was suggested that those Ti particles might be detached during the insertion of the implant [7,36] or released after insertion [14].

In the current study, SEM results showed Ti particles with a size of 0.5–5 μm in human jawbone marrow tissues. Previous studies reported that particles <1 μm could be taken up by non-phagocytic eukaryotic cells via endocytosis [37] and particles with diameters exceeding 0.75 μm can be taken up by macrophages, neutrophils and monocytes via phagocytosis or through macropinocytosis (>1 μm) by all cell types [38]. Therefore, transportation of Ti particles with size of 0.5–5 μm that were observed in human bone marrow tissues of present study into cells is possible. It should also be pointed out that a particle smaller than approximately 1 μm can no longer be seen by transmitted light microscopy.

In this study, bone marrow fibrosis, avital bone tissues and multinucleated cells were observed near the implant. Similarly, a previous post-mortem study about metal particles released from implants showed bone marrow fibrosis in lymph-node tissue [22]. Furthermore, multinucleated cells have been observed after hydroxyapatite implantation in rat periodontal tissues [39]. Bone marrow fibrosis might be induced by marrow injury and inflammation [40]. These effects are reported to be associated with surgical trauma during insertion of implants [41]. Multinucleated giant cells can be elicited by wear particles in periprosthetic tissues in human specimens and these cells might contain phagocytized wear particles [42]. These findings cited above are in accordance with the histological observations made in undecalcified, resin embedded human bone and implant sections in the present study.

5. Conclusion

Ti can be released into human jawbone and jawbone marrow tissues from dental implants. Compared to all other investigated isotopes only ^{47}Ti was observed in both the implants and human bone/bone marrow tissues near the implant but not in the control samples. The intensity of ^{47}Ti in human jawbone increased with decreasing distance to implant. Ti particles in size between 0.5 μm and 40 μm were observed in the jawbone marrow tissues near the implant, which might induce fibrosis and multinucleated cells. Based on our study with a small sample size we suggest that Ti dental implants might have no adverse clinical effects.

Acknowledgements

This study was financially supported by the China Scholarship Council (CSC, 201206220099). We would like to thank Mr. Peter Grill and Mr. Stefan Schulz for the technical support.

REFERENCES

[1] Lautenschlager EP, Monaghan P. Titanium and titanium alloys as dental materials. Int Dent J 1993;43:245–53.
[2] Elias C, Lima J, Valiev R, Meyers M. Biomedical applications of titanium and its alloys. JOM 2008;60:46–9.
[3] McCracken M. Dental implant materials: commercially pure titanium and titanium alloys. J Prosthodont 1999;8:40–3.
[4] Kasemo B. Biocompatibility of titanium implants: surface science aspects. J Prosthet Dent 1983;49:832–7.
[5] Schliephake H, Reiss G, Urban R, Neukam FW, Guckel S. Metal release from titanium fixtures during placement in the mandible: an experimental study. Int J Oral Maxillofac Implants 1993;8:502–11.
[6] Okabe T, Hero H. The use of titanium in dentistry. Cells Mater (USA) 1995;5:211–30.
[7] Franchi M, Bacchelli B, Martini D, Pasquale VD, Orsini E, Ottani V, et al. Early detachment of titanium particles from various different surfaces of endosseous dental implants. Biomaterials 2004;25:2239–46.
[8] Adya N, Alam M, Ravindranath T, Mubeen A, Saluja B. Corrosion in titanium dental implants: literature review. J Indian Prosthodont Soc 2005;5:127.
[9] Velasco-Ortega E, Jos A, Cameán AM, Pato-Mourelo J, Segura-Egea JJ. *In vitro* evaluation of cytotoxicity and genotoxicity of a commercial titanium alloy for dental implantology. Mutat Res/Genet Toxicol Environ Mutagen 2010;702:17–23.
[10] Meachim G, Williams D. Changes in nonosseous tissue adjacent to titanium implants. J Biomed Mater Res 1973;7:555–72.
[11] Galante JO, Lemons J, Spector M, Wilson Jr PD, Wright TM. The biologic effects of implant materials. J Orthop Res 1991;9:760–75.
[12] Hallab NJ, Mikecz K, Vermes C, Skipor A, Jacobs JJ. Orthopaedic implant related metal toxicity in terms of human lymphocyte reactivity to metal-protein complexes produced from cobalt-base and titanium-base implant alloy degradation. Mol Cell Biochem 2001;222:127–36.
[13] Hallab NJ, Jacobs JJ, Skipor A, Black J, Mikecz K, Galante JO. Systemic metal-protein binding associated with total joint replacement arthroplasty. J Biomed Mater Res 2000;49:353–61.
[14] Jacobs JJ, Gilbert JL, Urban RM. Current concepts review – corrosion of metal orthopaedic implants. J Bone Jt Surg 1998;80:268–82.
[15] Martini D, Fini M, Franchi M, Pasquale VD, Bacchelli B, Gamberini M, et al. Detachment of titanium and fluorohydroxyapatite particles in unloaded endosseous implants. Biomaterials 2003;24:1309–16.
[16] Edwin SH. Characteristics of trace ions released from embedded metal implants in the rabbit; 1962.
[17] Ducheyne P, Willems G, Martens M, Helsen J. In vivo metal-ion release from porous titanium-fiber material. J Biomed Mater Res 1984;18:293–308.
[18] Brien WW, Salvati EA, Betts F, Bullough P, Wright T, Rimnac C, et al. Metal levels in cemented total hip arthroplasty. A comparison of well-fixed and loose implants. Clin Orthop Relat Res 1992:66–74.

Please cite this article in press as: He X, et al. Analysis of titanium and other metals in human jawbones with dental implants – A case series study. Dent Mater (2016), http://dx.doi.org/10.1016/j.dental.2016.05.012

[19] Urban RM, Jacobs JJ, Tomlinson MJ, Gavrilovic J, Black J, Peoc'h M. Dissemination of wear particles to the liver, spleen, and abdominal lymph nodes of patients with hip or knee replacement. J Bone Jt Surg Am 2000;82:457–76.
[20] Sicilia A, Cuesta S, Coma G, Arregui I, Guisasola C, Ruiz E, et al. Titanium allergy in dental implant patients: a clinical study on 1500 consecutive patients. Clin Oral Implants Res 2008;19:823–35.
[21] Lalor PA, Revell PA, Gray AB, Wright S, Railton GT, Freeman MA. Sensitivity to titanium. A cause of implant failure? J Bone Jt Surg Br 1991;73:25–8.
[22] Case CP, Langkamer VG, James C, Palmer MR, Kemp AJ, Heap PF, et al. Widespread dissemination of metal debris from implants. J Bone Jt Surg Br 1994;76:701–12.
[23] Amstutz HC, Campbell P, Kossovsky N, Clarke IC. Mechanism and clinical significance of wear debris-induced osteolysis. Clin Orthop Relat Res 1992:7–18.
[24] Dannenmaier WC, Haynes DW, Nelson CL. Granulomatous reaction and cystic bony destruction associated with high wear rate in a total knee prosthesis. Clin Orthop Relat Res 1985;22:4–30.
[25] Kim JH, Jung Y, Kim BS, Kim SH. Stem cell recruitment and angiogenesis of neuropeptide substance P coupled with self-assembling peptide nanofiber in a mouse hind limb ischemia model. Biomaterials 2013;34:1657–68.
[26] Milz S, Putz R. Quantitative morphology of the subchondral plate of the tibial plateau. J Anat 1994;185:103–10.
[27] Gruhl S, Witte F, Vogt J, Vogt C. Determination of concentration gradients in bone tissue generated by a biologically degradable magnesium implant. J Anal Atomic Spectrom 2009;24:181–8.
[28] Niinomi M. Metals for biomedical devices. Elsevier; 2010.
[29] Rae T. The toxicity of metals used in orthopaedic prostheses. An experimental study using cultured human synovial fibroblasts. J Bone Jt Surg Br Vol 1981;63:435–40.
[30] Saquib Q, Al-Khedhairy AA, Siddiqui MA, Abou-Tarboush FM, Azam A, Musarrat J. Titanium dioxide nanoparticles induced cytotoxicity, oxidative stress and DNA damage in human amnion epithelial (WISH) cells. Toxicol In Vitro 2012;26:351–61.
[31] He X, Hartlieb E, Rothmund L, Waschke J, Wu X, Van Landuyt KL, et al. Intracellular uptake and toxicity of three different titanium particles. Dent Mater 2015;31:734–44.
[32] Himmlova L, Dostalova T, Kacovsky A, Konvickova S. Influence of implant length and diameter on stress distribution: a finite element analysis. J Prosthet Dent 2004;91:20–5.
[33] Baggi L, Cappelloni I, Di Girolamo M, Maceri F, Vairo G. The influence of implant diameter and length on stress distribution of osseointegrated implants related to crestal bone geometry: a three-dimensional finite element analysis. J Prosthet Dent 2008;100:422–31.
[34] Prohaska T, Latkoczy C, Schultheis G, Teschler-Nicola M, Stingeder G. Investigation of Sr isotope ratios in prehistoric human bones and teeth using laser ablation ICP-MS and ICP-MS after Rb/Sr separation. J Anal Atomic Spectrom 2002;17:887–91.
[35] Kang D, Amarasiriwardena D, Goodman AH. Application of laser ablation-inductively coupled plasma-mass spectrometry (LA-ICP-MS) to investigate trace metal spatial distributions in human tooth enamel and dentine growth layers and pulp. Anal Bioanal Chem 2004;378: 1608–15.
[36] Flatebo RS, Hol PJ, Leknes KN, Kosler J, Lie SA, Gjerdet NR. Mapping of titanium particles in peri-implant oral mucosa by laser ablation inductively coupled plasma mass spectrometry and high-resolution optical darkfield microscopy. J Oral Pathol Med 2011;40:412–20.
[37] Rejman J, Oberle V, Zuhorn IS, Hoekstra D. Size-dependent internalization of particles via the pathways of clathrin- and caveolae-mediated endocytosis. Biochem J 2004;377:159–69.
[38] Conner SD, Schmid SL. Regulated portals of entry into the cell. Nature 2003;422:37–44.
[39] Kawaguchi H, Ogawa T, Shirakawa M, Okamoto H, Akisaka T. Ultrastructural and ultracytochemical characteristics of multinucleated cells after hydroxyapatite implantation into rat periodontal tissue. J Periodontal Res 1992;27:48–54.
[40] Travlos GS. Histopathology of bone marrow. Toxicol Pathol 2006;34:566–98.
[41] Piattelli A, Piattelli M, Mangano C, Scarano A. A histologic evaluation of eight cases of failed dental implants: is bone overheating the most probable cause. Biomaterials 1998;19:683–90.
[42] Anazawa U, Hanaoka H, Morioka H, Morii T, Toyama Y. Ultrastructural cytochemical and ultrastructural morphological differences between human multinucleated giant cells elicited by wear particles from hip prostheses and artificial ligaments at the knee. Ultrastruct Pathol 2004;28:353–9.

Please cite this article in press as: He X, et al. Analysis of titanium and other metals in human jawbones with dental implants – A case series study. Dent Mater (2016), http://dx.doi.org/10.1016/j.dental.2016.05.012